communications biology

A Nature Portfolio journal

Article

https://doi.org/10.1038/s42003-025-07899-y

A chromatin-focused CRISPR screen identifies USP22 as a barrier to somatic cell reprogramming

Gülben Gürhan[1,5], Kenan Sevinç[1,5], Can Aztekin[1], Mert Gayretli[1], Alperen Yılmaz[1], Abdullah Burak Yıldız[1], Elif Naz Ervatan[1], Tunç Morova[1,2], Elif Datlı[1], Oliver D. Coleman[3], Akane Kawamura[3], Nathan A. Lack[1,2], Hamzah Syed[1,4] & Tamer Önder[1]

Cell-autonomous barriers to reprogramming somatic cells into induced pluripotent stem cells (iPSCs) remain poorly understood. Using a focused CRISPR-Cas9 screen, we identified Ubiquitin-specific peptidase 22 (USP22) as a key chromatin-based barrier to human iPSC derivation. Suppression of USP22 significantly enhances reprogramming efficiency. Surprisingly, this effect is likely to be independent of USP22's deubiquitinase activity or its association with the SAGA complex, as shown through module-specific knockouts, and genetic rescue experiments. USP22 is not required for iPSC derivation or maintenance. Mechanistically, USP22 loss during reprogramming downregulates fibroblast-specific genes while activating pluripotency-associated genes, including *DNMT3L*, *LIN28A*, *SOX2*, and *GDF3*. Additionally, USP22 loss enhances reprogramming efficiency under naïve stem cell conditions. These findings reveal an unrecognized role for USP22 in maintaining somatic cell identity and repressing pluripotency genes, highlighting its potential as a target to improve reprogramming efficiency.

Expression *OCT4*, *SOX2*, *KLF4*, and *MYC* (OSKM) can reprogram somatic cells into induced pluripotent stem cells (iPSCs)[1,2]. Reprogramming is characterized by distinct phases in which a series of cellular and molecular transitions takes place[3]. In the initial phase, cell proliferation increases, somatic transcription program is downregulated and mesenchymal-to-epithelial transition occurs[4,5]. During the maturation stage, developmental genes are transiently upregulated and pluripotency-associated genes are turned on. At the end of reprogramming, pluripotency network is stabilized and emerging iPSCs become transgene-independent[6]. iPSC generation efficiency from human adult somatic cells such as fibroblasts is lower than 0.1% even when OSKM factors are provided to each cell at high copy number[7]. This observation suggests that there are intrinsic, cell-autonomous barriers to reprogramming. Identification of such barriers may uncover mechanisms that control cell proliferation, maintain cellular identity, or actively repress pluripotency[8–10].

USP22 is a member of the deubiquitinase module of SAGA (SPT-ADA-GCN5 acetylase) complex[11]. SAGA complex is conserved from yeast to human and regulates gene expression through histone modifications and recruitment of transcription machinery[12–14]. It consists of more than 20 proteins grouped in 5 major modules: histone acetylation module (HAT), core module, TF- (transcription factor) binding module, deubiquitination module (DUB) and splicing module[15,16]. Although USP22 contains zinc-finger and deubiquitinase domains, it does not have deubiquitinase activity by itself[17–20]. USP22 requires additional regulatory proteins such as ATXN7L3 and ENY2 for its enzymatic activity and ATXN7 for coupling to the remainder modules of SAGA complex[18,21]. USP22 has both histone (H2B) and non-histone protein targets[22–26] and several reports indicate that DUB module may function independently from SAGA complex[16,27].

USP22 has been studied in the context of mouse embryonic development[26,28], pluripotency exit[29] and extra-embryonic lineage differentiation[28,30]. USP22 null mouse embryos cannot undergo full development. USP22 knockout embryos start to die at E9.5 and at E14.5 no embryos remain alive, pointing to an essential role for USP22 during mouse development[28]. In mouse embryonic stem cells (mESC), USP22 knockdown upregulates SOX2 expression and attenuates the induction of differentiation marker genes in embryoid body formation assays[29]. These results suggest that USP22 controls pluripotency exit and differentiation into three germ

[1]School of Medicine, Koç University, Istanbul, Turkey. [2]Vancouver Prostate Centre, Department of Urologic Science, University of British Columbia, Vancouver, BC, Canada. [3]Chemistry - School of Natural and Environmental Sciences, Newcastle University, Newcastle, United Kingdom. [4]Biostatistics, Bioinformatics and Data Management Core, KUTTAM, Koç University, Istanbul, Turkey. [5]These authors contributed equally: Gülben Gürhan, Kenan Sevinç.
e-mail: tonder@ku.edu.tr

layers through its deubiquitinase activity. Additional USP22 KO phenotypes in the mouse are failure to develop proper vasculature in placenta[28] and abnormalities in intestinal epithelial lineage specification[30]. These results may explain the embryonic-lethality phenotype of USP22 knockout in mice. However, to date, the role of USP22 in human development and differentiation has not been investigated.

Previous studies have demonstrated that epigenetic factors, which activate gene transcription, can serve as impediments to cellular reprogramming by preserving the identity of somatic cells. For instance, inhibition of factors such as SUMO, FACT, RPAP1, BRD9, and CBP/EP300 have all been shown to facilitate somatic cell reprogramming[8,31–35]. Conversely, the inhibition of epigenetic factors that suppress gene expression, such as DNA methylation, H3K9 methylation, and histone deacetylation, enhances reprogramming efficiency by promoting the activation of the pluripotency network[31,36–39]. Recent genetic screens employing CRISPR-Cas9-based approaches have identified barriers to cell fate conversions[40–42]. These findings motivated us to conduct a chromatin-focused knockout screen during reprogramming of human somatic cells. This screen revealed USP22 as a barrier to reprogramming for human pluripotency.

Results

EpiDoKOL screen identified USP22 as a barrier to human somatic cell reprogramming

To interrogate the function of chromatin factors in reprogramming we constructed a focused CRISPR-sgRNA library (Epigenetic Domain-specific Knockout Library (EpiDoKOL)), targeting the functional domains of such genes[43]. EpiDoKOL consists of 1750 sgRNAs in total, targeting 247 different genes, and 80 non-targeting controls[44]. Human fibroblast cells stably expressing Cas9 were transduced by pooled viral library at low MOI and reprogrammed to induced pluripotent stem cells by overexpressing *OCT4*, *SOX2*, *KLF4*, and *MYC* factors. TRA-1-60 positive cells at day 21 of reprogramming were sorted out to compare pluripotency-enriched gRNAs to the initial representation of gRNAs prior to reprogramming (Fig. 1A). The screen was done in the presence of a DOT1L inhibitor (EPZ004777) to elevate the basal reprogramming efficiency and to identify factors which would act additively to increase reprogramming efficiency[38]. We used Model-based Analysis of Genome-wide CRISPR/Cas9 Knockout (MAGeCK) algorithm[43] to analyze the screen data which identified *DNMT3A*, *PAXIP1*, *EP300*, and *USP22* targeting gRNAs to be significantly enriched in TRA-1-60 positive cells (Figs. 1B, S1A). DNMT3A and EP300 are known barriers to reprogramming, whereas PAXIP1 and USP22 were not previously associated with reprogramming[38,45,46]. In validation experiments with individual gRNAs, PAXIP1 targeting gRNAs failed to increase reprogramming efficiency and were considered false positives. However, multiple independent gRNAs against USP22 significantly increased the efficiency of reprogramming (Fig. 1C).

To investigate the role of USP22 in reprogramming independently of DOT1L inhibition, *USP22* was targeted by three independent gRNAs and its depletion was confirmed at the protein level (Fig. 1D). When these cells were reprogrammed to iPSCs, the reprogramming efficiency increased up to 3-fold compared to non-targeting gRNA expression (Fig. 1E). To address if

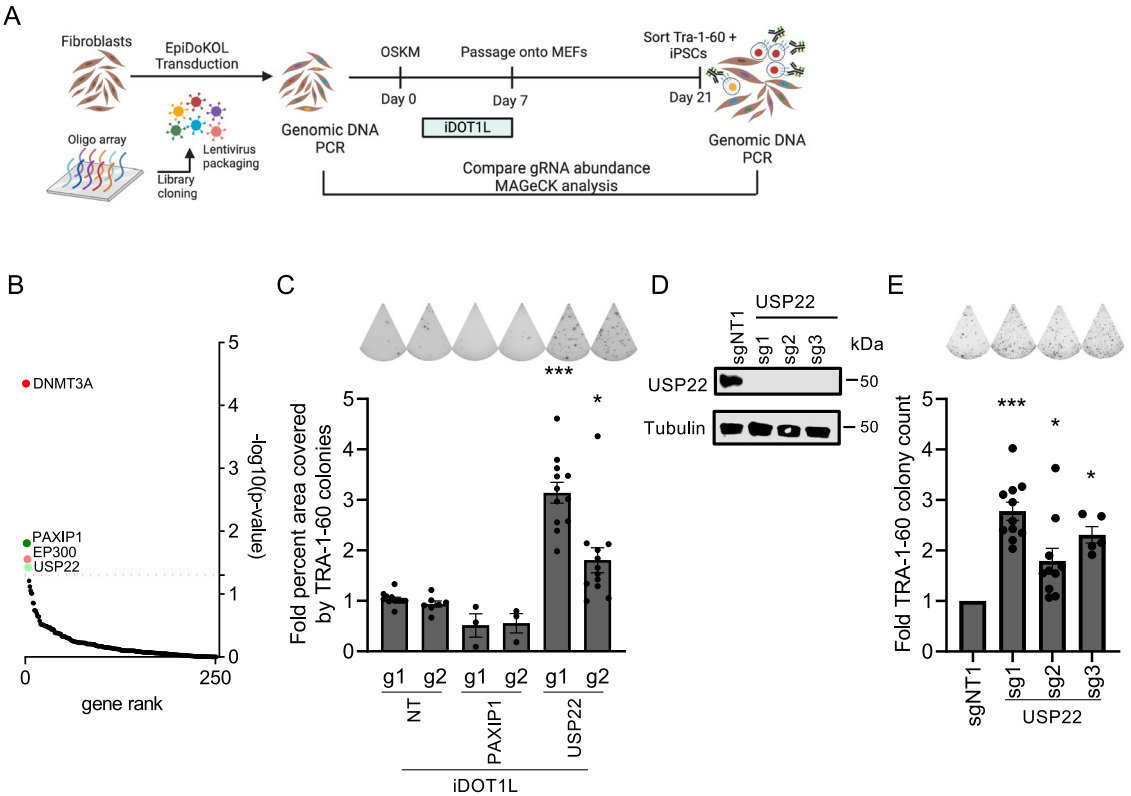

Fig. 1 | EpiDoKOL screen identified USP22 as a barrier to human somatic cell reprogramming. A Schematic representation of the screen outline. **B** Positively selected gRNAs during reprogramming identified by MAGeCK algorithm at the gene level. Created in BioRender. Onder, T. (2025) https://BioRender.com/j82z183. **C** Fold change in reprogramming efficiency upon gRNA expression. Triangular images above the bars are sections of representative Tra-1-60-stained wells. Error bars indicate the error of mean. $n = 3$, independent experiments were conducted for PAXIP1 gRNA expression and $n = 12$, independent experiments for USP22 gRNA expression. Two-sided *t*-test *p*-values 0.0001 and 0.0081 for USP22 g1 and g2, respectively, and 0.1685 and 0.1466 for PAXIP1 g1 and g2, respectively. **D** Western blot image showing USP22 protein level of USP22 targeting gRNAs in fibroblasts. Tubulin was used as a loading control. **E** Fold change in reprogramming efficiency upon USP22 targeting gRNA expression. Triangular images above the bars are sections of representative Tra-1-60-stained wells. Error bars indicate the error of mean. $n = 11$, independent experiments were conducted for USP22 sg1 expression, $n = 10$ for USP22 sg2 expression and $n = 5$ for USP22 sg3 expression. Two-sided t-test to compare g1, g2, and g3 to the gNT1 gives following *p*-values 0.0001, 0.0111, and 0.0013, respectively.

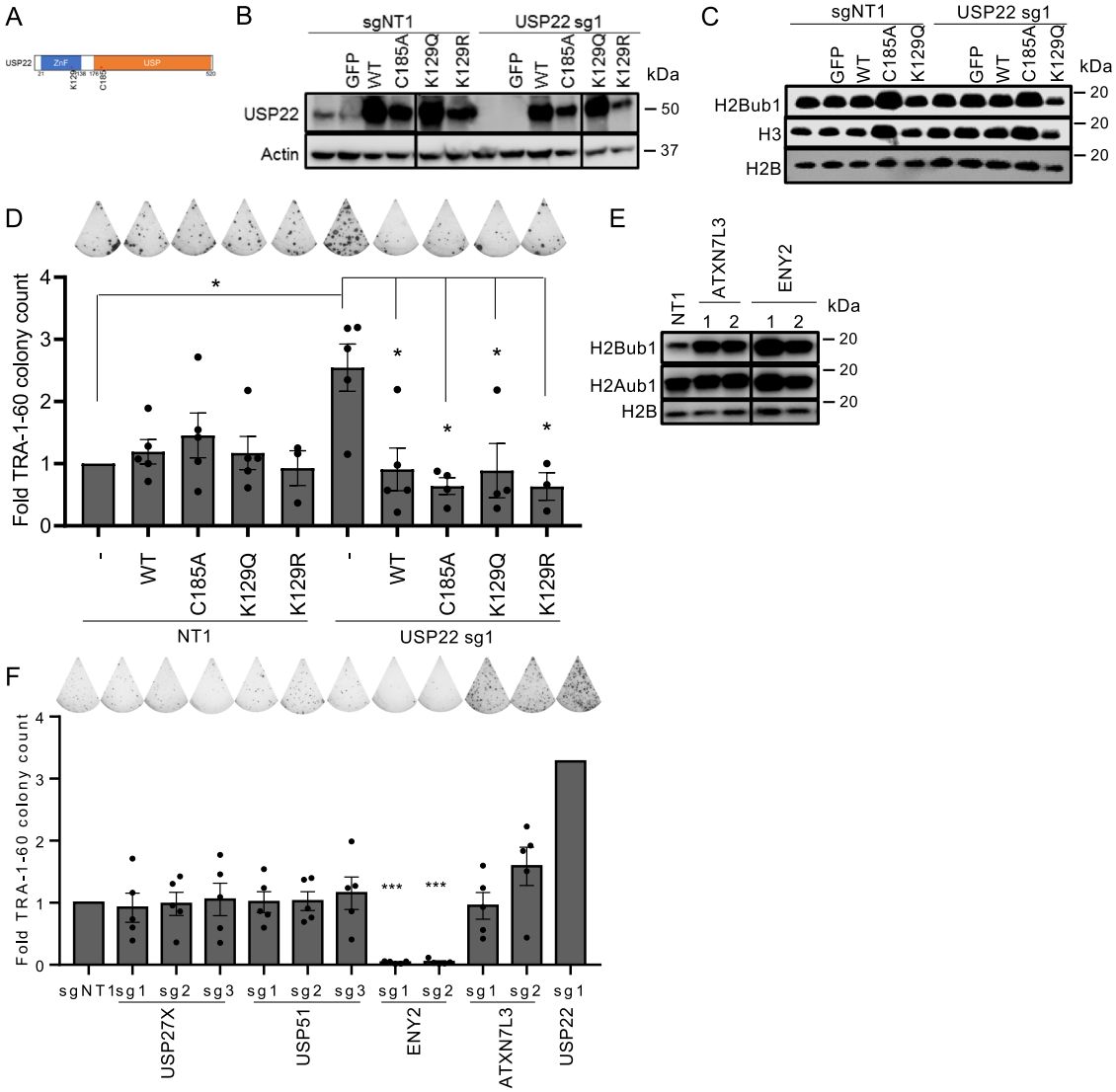

Fig. 2 | Catalytic activity of USP22 is not a barrier to reprogramming. A Diagram showing USP22 domains and mutated amino acid positions. **B** Western blot image showing USP22 protein levels after USP22 overexpressions in both non-targeting and USP22 targeting gRNA expressing fibroblasts. Actin was used as a loading control. **C** Western blot image showing H2Bub protein levels after USP22 overexpressions in both non-targeting and USP22 targeting gRNA expressing fibroblasts. Histones H3 and H2B were used as loading controls. **D** Fold change in reprogramming efficiency upon USP22 overexpressions in both wild-type and USP22 knockout background. Triangular images above the bars are sections of representative Tra-1-60-stained wells. Error bars indicate the error of mean. $n = 3$, independent experiments for KR mutations, $n = 4$ for CA and KQ mutations in USP22 knockout background, and $n = 5$ for other comparisons. Two-sided t-test was performed between sgNT1 and USP22 sg1 without any overexpression and p-value is 0.0153. Two-sided t-test was performed between USP22 sg1 expressing cells without overexpression and WT, C185A, K129Q, and K129R and p-value is 0.0129, 0.0054, 0.0264, and 0.0052, respectively. **E** Western blot image showing H2Bub and H2Aub protein levels after ATXN7L3 or ENY2 knockouts in fibroblasts. H2B was used as a loading control. **F** Fold change in reprogramming efficiency upon ATXN7L3, ENY2, USP27X, or USP51 knockouts. Triangular images above the bars are sections of representative Tra-1-60-stained wells. Error bars indicate the error of mean. $n = 5$, independent experiments. Two-sided t-test shows p-value smaller than 0.0001 for ENY2 sg1 and sg2 compared to sgNT1.

this increased reprogramming efficiency phenotype is cell strain- or OSKM delivery method-specific, we reprogrammed an additional human adult fibroblast strain with episomal vectors (Fig. S1B). The reprogramming efficiency increased 3-fold upon *USP22* knockout (Fig. S1C). Treatment of these primary cells with a DOT1L inhibitor had an additive effect, resulting in more than 10-fold increase in reprogramming efficiency (Fig. S1C). Using three additional primary fibroblasts from independent donors we verified the reprogramming effect (Fig. S1D, E). Taken together, these results show that USP22 acts as an important barrier to reprogramming of somatic cells to pluripotency.

Catalytic activity of USP22 is not a barrier to reprogramming

To determine if USP22's barrier function depends on its deubiquitinase activity, we performed genetic rescue experiments in the context of reprogramming by overexpressing either wild-type or C185A deubiquitinase mutant USP22 cDNAs in USP22 KO cells[47] (Fig. 2A, B). As we wanted to understand the barrier role of USP22 in reprogramming rather than its additive effect with DOT1L inhibition, we omitted the DOT1L inhibitor for these experiments. Interestingly, levels of Histone H2B mono-ubiquitination (H2Bub), a reported target of USP22, did not change in USP22 KO cells compared to control cells, suggesting the presence of alternative, redundant DUBs for this target (Fig. 2C). Overexpression of wildtype USP22 did not decrease global H2Bub levels, but the catalytic dead C185A mutant resulted in a modest increase (Fig. 2C). Importantly, both the wildtype and C185A mutant were able to suppress the formation of iPSCs and rescue the increased reprogramming phenotype of USP22 KO (Fig. 2D). These results point to a deubiquitinase-independent role for USP22 in blocking reprogramming.

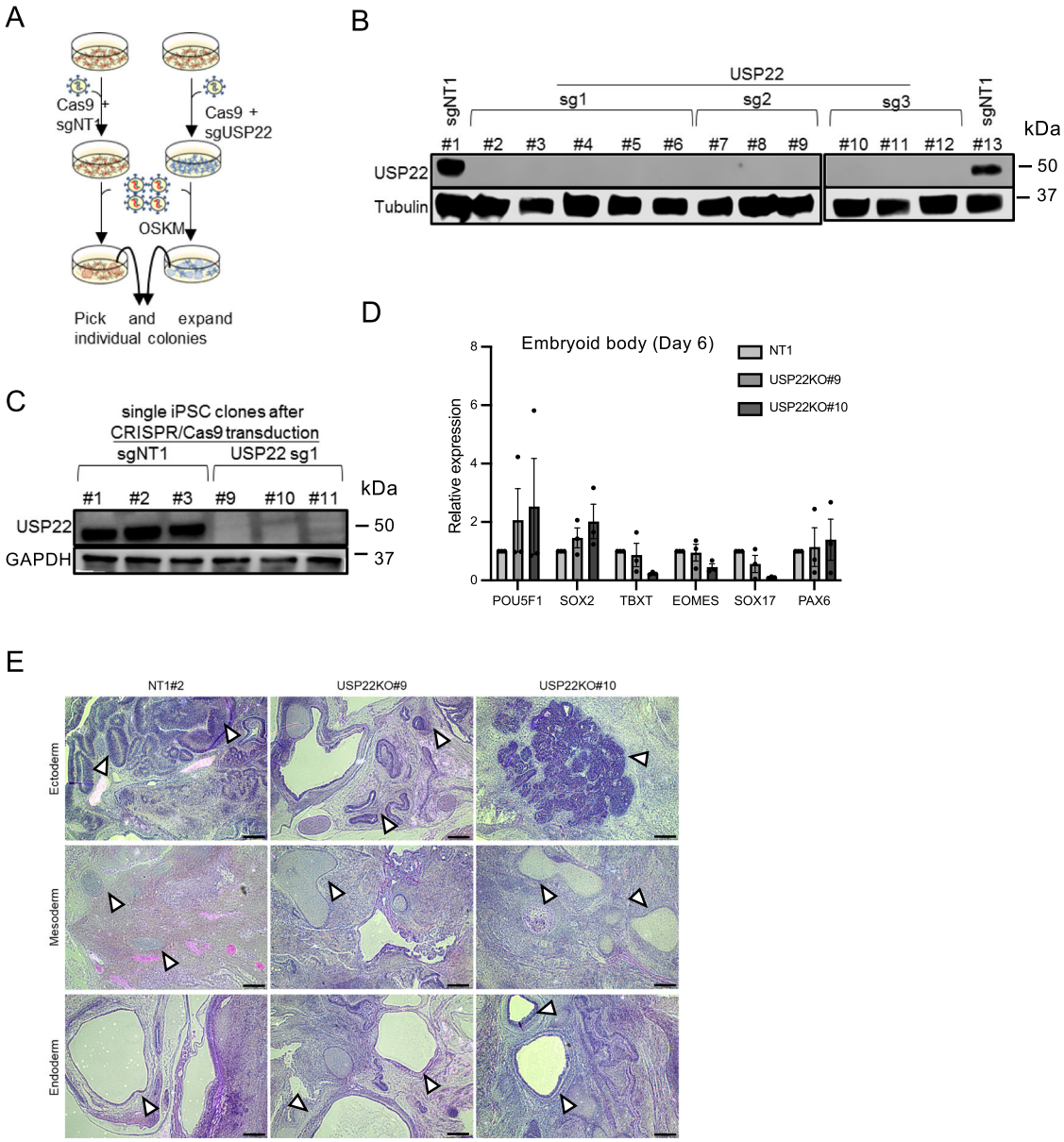

Fig. 3 | USP22 loss results in differentiation defects. A Schematic representation of generating USP22 knockout iPSC clones used in Fig. 3B. **B** Western blot image showing USP22 protein levels in iPSCs generated from Cas9 and USP22 targeting gRNA expressing fibroblasts. Tubulin was used as a loading control. **C** Western blot image showing USP22 protein levels in iPSC clones generated from Cas9 and USP22 targeting gRNA expressing iPSCs. Tubulin was used as a loading control. **D** Relative expression levels of lineage markers upon EB formation for NT1#2, USP22KO#9-10. **E** Hematoxylin and eosin-stained sections of teratomas of NT1#2, USP22KO#9-10 iPSCs. Arrowheads point to representative tissues from endoderm (glandular epithelium), ectoderm (neuroepithelium), and mesoderm (cartilage) lineages. 2 mice were injected per cell line.

We next asked if association of USP22 with the SAGA complex is important in the context of reprogramming. Acetylation of K129 on USP22 can regulate its enzymatic activity as well as its binding to GCN5[48]. K129R (acetylation deficient) or K129Q (acetylation mimic) mutant were both able to rescue the USP22 KO phenotype (Fig. 2D), suggesting that regulation of USP22 incorporation into SAGA complex is unlikely to play an important role in blocking reprogramming. To directly assess the function of the SAGA deubiquitinase module, we targeted two of its critical components, *ENY2* and *ATXN7L3*[21]. As expected, global histone ubiquitination levels increased upon expression of sgRNAs targeting these two genes (Fig. 2E). However, *ATXN7L3* knockout did not have any effect on reprogramming efficiency whereas *ENY2* knockout completely blocked iPSC generation (Fig. 2F). USP27X and USP51 have been shown to compete with USP22 and couple with ATXN7L3 and ENY2[49]. Knocking out USP22 competitor deubiquitinases *USP27X* or *USP51* did not affect reprogramming (Figs. 2F, S2A). Treatment with a recently developed cyclic peptide inhibitor of USP22 (hD1) during reprogramming did not increase the reprogramming efficiency[50], although it also did not affect overall H2Bub levels (Fig. S2B, C). These results suggest that USP22 acetylation, incorporation into SAGA, or its deubiquitinase activity is unlikely contribute to its role as a barrier to reprogramming.

USP22 is dispensable for maintaining pluripotency

To assess the effect of *USP22* knockout on human iPSCs, we picked and expanded colonies generated from *USP22* gRNA and Cas9 expressing fibroblasts (Fig. 3A). USP22 protein was absent in all clones (11 out of 11) tested, indicating that its loss is compatible for iPSC generation (Fig. 3B). In a complementary approach, we knocked out *USP22* in a control, transgene-free hiPSC line[51] by infecting it with USP22 gRNA vectors and picking single cell clones. All three USP22 KO hiPSC clones could be maintained in culture in an undifferentiated state, indicating that USP22 does not impair self-renewal (Fig. 3C). To assess pluripotency, we performed embryoid body

formation assay and observed that USP22 KO clones retained higher levels of undifferentiated state markers, *POU5F1* and *SOX2* on day 6 compared to the control parental line. In addition, one of the USP22 KO clones failed to robustly activate mesoderm and endoderm markers *TBXT*, *EOMES*, and *SOX17* (Fig. 3D). However, USP22 KO clones could still form teratomas that contained cells derived from three germ layers, suggesting that USP22 does not completely block differentiation ability (Fig. 3E). Taken together these results suggested USP22 is not critical for self-renewal of human iPSCs and that it may have a repressive effect on pluripotency genes during differentiation.

USP22 stabilizes maturation stage of reprogramming for faithful pluripotency acquisition

To understand how USP22 loss increases reprogramming, we first measured the proliferation rate in USP22 KO fibroblasts and observed that it was not changed before or during reprogramming compared to control cells (Fig. S3A). Next, we determined the percentage of TRA-1-60 positive cells at the early time point of 6 days after OSKM transduction to assess if reprogramming was accelerated in the absence of USP22. DOT1L inhibition increased the number of TRA-1-60 positive cells on day 6 as expected, but *USP22* knockout had no effect (Fig. S3B). As the number of TRA-1-60 cells was similar across control and *USP22* knockout cells on day 6 of reprogramming, we performed bulk RNA sequencing at this time-point to uncover the transcriptional changes caused by USP22 loss before the emergence of reprogrammed cells. We observed that control and USP22 knockout replicate RNA samples were well correlated (Fig. S3C). Loss of USP22 during reprogramming led to upregulation of 226 genes and downregulation of 442 genes (Fig. 4A).

We hypothesized that USP22 loss enhances reprogramming by facilitating the activation of pluripotency genes and repression of differentiation-related genes. To test this hypothesis, we first assessed the genesets enriched among differentially downregulated genes. Accordingly, epithelial-to-mesenchymal transition (EMT), extracellular matrix, cell adhesion, and cell motility genes were most downregulated among all Hallmark and Gene Ontology sets interrogated. (Fig. 4B, C). Many mesenchyme-specific genes such as *FOXC2*, *COL1A2*, *POSTN*, *VIM*, and *DCN* were significantly downregulated in USP22 KO cells (Figs. 4A, S3E). These results suggest that USP22 plays a role in maintaining somatic cell identity. Next, we focused on genesets enriched among differentially upregulated genes which revealed that cell cycle related genes, apoptosis, epithelium development, and cytoskeleton organization genes were most upregulated upon USP22 loss (Fig. 4B). Targets of pluripotency-related transcription factors such as *SOX2*, *SALL4*, *MYC* and *NANOG* were enriched in upregulated genes in USP22 KO cells (Fig. S3D). Similarly, gene set enrichment analysis (GSEA) showed negative enrichment for fibroblast-related genes upon USP22 loss whereas pluripotency-related genes were positively enriched (Fig. 4D). Several genes previously identified to be late markers of reprograming such as *GDF3* and *SOX2* were upregulated in USP22 KO cells 6 days after OSKM expression[52]. We confirmed upregulation of endogenous pluripotency genes in USP22 KO cells across later time points as well (day 9 to 12) (Figs. 4E, S3F). Notably, wildtype or catalytic dead mutant USP22 expression in the knockout background reverted the reprogramming associated upregulation of pluripotency genes (Fig. 4E). We also observed that USP22 loss upregulated genes associated with naïve pluripotency such as *DNMT3L*, ALPPL2[53,54]. Therefore, we next asked if USP22 inhibition can facilitate reprogramming to a naïve-like pluripotent state. Indeed, under naïve culture conditions, USP22 KO cells generated two-fold more Tra-1-60 and KLF17+ colonies than control fibroblasts (Fig. 4F). USP22 KO cells reprogrammed under naïve conditions expressed naïve markers such as *DPPA5*, *ALLPL2*, *KLF17* while downregulating prime marker such as *CD24* and *DUSP6* (Fig S4G). These results show that USP22 loss results in enhanced reprogramming under both primed and naïve conditions and point to a suppressive effect of USP22 on the expression of multiple endogenous pluripotency factors.

Discussion

In this study, we performed a chromatin focused CRISPR screen during human somatic cell reprogramming. In addition to confirming previously identified barriers to reprogramming, such as DNMT3A and EP300[36,37,39,45,55], this screen uncovered a reprogramming barrier, USP22. A previous survey of USP family members in murine reprogramming did not identify USP22 as hit[56]. Similarly, large-scale CRIPSR screen in MEFs did not identify as reprogramming barrier[57,58]. Although not directly tested in the present work, USP22 may be a species-specific barrier to human somatic cell reprogramming. We validate USP22's suppressive effects on human iPSC generation across independent fibroblast lines and OSKM delivery methods. Importantly, the combinatorial loss of USP22 and inhibition of DOT1L, a factor we previously identified to be a major barrier to reprogramming, led to a striking tenfold increase in reprogramming efficiency of human cells.

To understand how USP22 suppresses reprogramming we first investigated whether its deubiquitinase activity is important. Notably, application of a cyclic peptide inhibitor targeting USP22, previously reported to influence H2B ubiquitination, did not yield a discernible change in reprogramming efficiency. Similarly, in genetic rescue experiments, we observed that expression of a catalytically dead mutant USP22 could still suppress the enhanced reprogramming phenotype of USP22 knockout cells. It would be interesting to test if selective degradation of USP22 using PROTACs could increase the efficiency of reprogramming and potentially be incorporated into chemical-only reprogramming protocols[59–61]. In addition to its catalytic activity, we also considered whether USP22 blocks reprogramming via its involvement in the SAGA complex. Knockouts of additional members of the SAGA DUB modules, ATXN7L3 and ENY2, or potential USP22 replacements in the DUB module USP27X or USP51[49], also did not improve reprogramming efficiency. We observed that ENY2 is absolutely required for iPSC generation which could be due to its involvement in TREX complex mediated RNA export[62,63]. Our results, therefore, point to a SAGA-independent role for USP22 in preventing reprogramming. This is consistent with a critical role for the SAGA complex in reprogramming, where histone acetyltransferase Gcn5 has been found to be required[14]. In the future, it will be interesting to identify USP22's protein interaction partners, other than SAGA, which could shed light on the mechanism by which it impedes reprogramming.

Using USP22 knockout hiPSCs, we find that USP22 is dispensable for pluripotency and self-renewal of human PSCs. CRISPR and CRISPRi screens have shown that suppressing USP22 may increase fitness of ESCs and iPSCs[64,65]. In mice, *USP22* deletion is embryonic lethal and causes defects in placental and kidney vascularization[28,30]. *USP22* knockout hiPSCs were able to form teratomas containing cells representative of all three germ layers, indicating that USP22 is not required for differentiation in this assay. However, in embryoid body formation assays, we observed higher levels of *OCT4* and *SOX2* remaining in USP22 knockouts, as well as a failure to robustly induce mesoderm and endoderm markers SOX17 and EOMES. Investigating the role of USP22 in differentiation of human PSCs using newly developed models such as gastruloids may yield further insights on its role in facilitating exit from pluripotency[66,67].

The results presented in this work do not eliminate the possibility that USP22 knockout has indirect barrier role in reprogramming. One possibility is that the integrity of the SAGA complex or its chromatin localization may be disrupted. We have also not addressed whether the zinc finger domain which may be important in protein-protein interactions of USP22 is important. It will be relevant to investigate this domain's barrier role in reprogramming in the future and relevant interactors. Second, USP22 may be a general factor in maintaining pluripotency[29]. Although we observed that USP22 knockout iPSCs can differentiate into three germ layers, it would be interesting to show USP22's role in human pluripotency exit and whether it is affected by the catalytic activity of the enzyme. Third, USP22 knockout may destabilize the SAGA complex at certain chromatin loci and lead to indirect transcriptional effects. To test this, chromatin localization of USP22 during reprogramming needs to be evaluated[29].

Our transcriptome data shows that USP22 deletion upregulates pluripotency-related genes including *SOX2*, *ESRG*, and *GDF3*, and naïve pluripotency-marker genes such as *DNMT3L, ALPPL2*, and *KLF5*. On the other hand, mesenchyme-related gene sets and fibroblast-specific gene sets were negatively correlated with USP22 loss. Additionally, genes encoding various collagens were downregulated upon USP22 loss during reprogramming. *COL1A1* and *COL11A1* were previously shown to be barriers to cellular reprogramming[68,69]. Overall, these results show that USP22 is

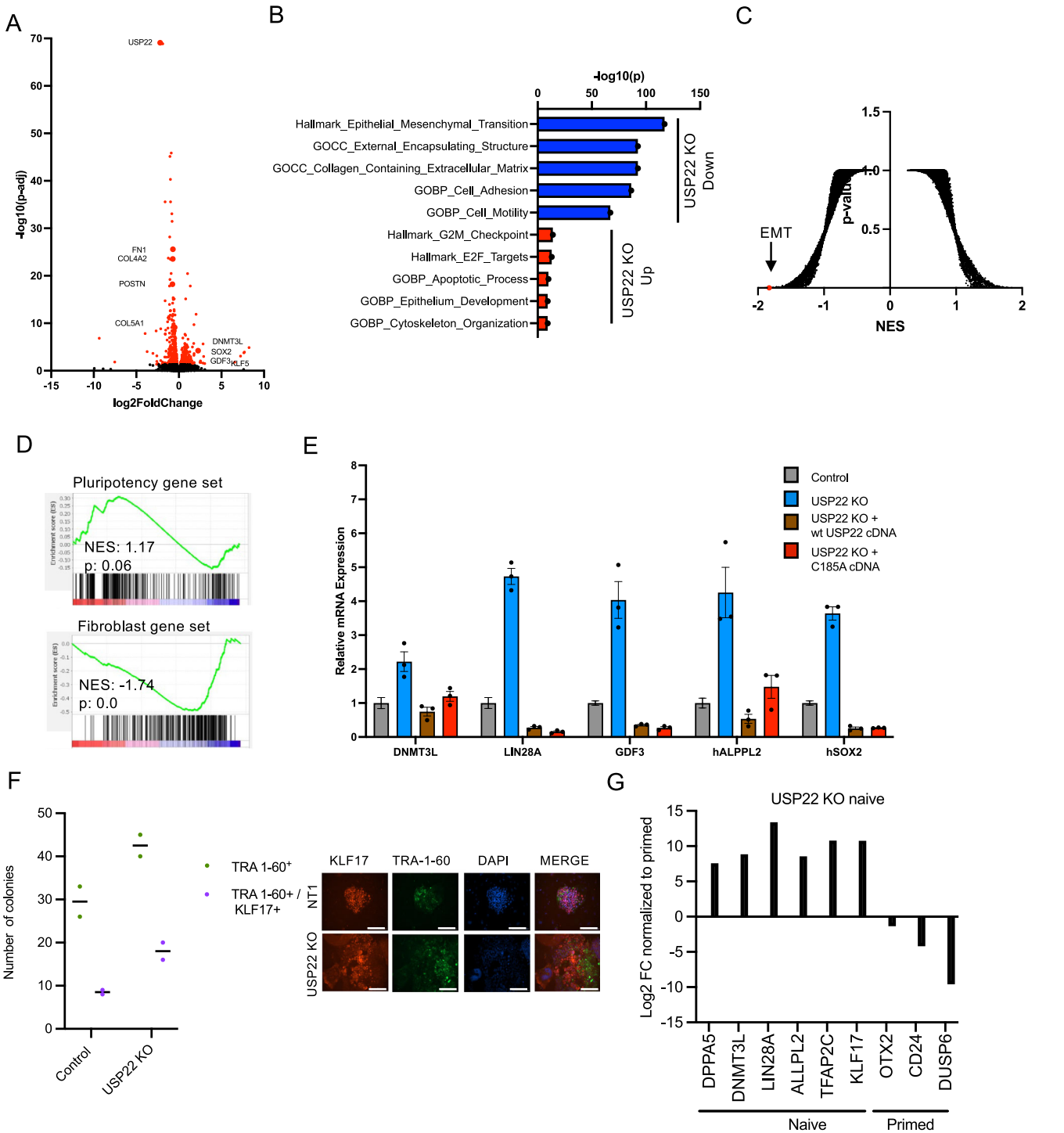

Fig. 4 | USP22 loss stabilizes pluripotency network during reprogramming. **A** Volcano-plot of RNA-seq data comparing USP22 KO and control cells during reprogramming. **B** Gene ontology analysis for differentially regulated genes upon USP22 knockout. Top 5 upregulated and downregulated gene sets are shown. **C** GSEA p-value and normalized enrichment scores on pre-ranked gene lists according to log2FC value for comparisons of reprogramming fibroblasts expressing USP22 gRNA to NT1 for all gene sets available at The Molecular Signatures Database (mSigDB). **D** GSEA results for pluripotency- and fibroblast-related gene sets upon USP22 loss during reprogramming. **E** Relative expression levels of pluripotency-associated genes on day 9 of reprogramming in control (NT1), USP22 KO cells expressing either wild-type or catalytic dead mutant USP22 cDNAs. $n = 3$ biological replicates with two technical replicates each. **F** Number of Tra-1-60- and/or KLF17-positive colonies generated under naïve conditions (PGXL) from control or USP22 KO fibroblasts. Immunofluorescence images of KLF17 and TRA-1-60-stained cells are shown below. **G** Relative expression of naïve and primed makers in USP22 KO cells after reprogramming under naïve PSC culture conditions. Expression values are normalized to primed PSCs.

necessary to maintain fibroblast gene expression and suppresses pluripotency network during reprogramming. USP22 has been shown to be an essential gene for naïve stem cell maintenance[70]. However, in the context of reprogramming, loss of USP22 enhances naïve marker expression such as *KLF5* and *DNMT3L*, and under naïve culture conditions USP22 knockout fibroblasts from greater numbers of KLF17-positive naïve-like iPSCs. Therefore, our findings indicate that USP22 may act as a general barrier to reprogramming.

Materials and methods

Cell culture

HEK293T cells were maintained in D10 Medium (DMEM (Gibco) containing, 10% FBS (Gibco), and 1% Penicillin-Streptomycin (Gibco)). dH1f cells, generated by differentiation of H1 ESCs (CVCL_9771) as previously described[38], were maintained in either in D10 Medium or in α-MEM Medium (Alpha-MEM (Lonza) containing, 10% FBS (Gibco), 1% Penicillin-Streptomycin (Gibco) and 1% Non-essential amino acids (Gibco)). Induced pluripotent stem cells were maintained in human ES medium (DMEM/F12 (Lonza), 20% KOSR (knock-out serum replacement) (Gibco), 10 ng/ml bFGF, 0.1 mM β-mercaptoethanol, 1% non-essential amino acids, 1% Penicillin/Streptomycin).

Generation of inactivated MEFs

MEFs were isolated from E13.5 embryos generated by timed matings of C57BL/6 mice. Confluent cultures at passage 4 or 5 were washed once with PBS and treated with 10 µg/mL mitomycin C (in 10% FBS, 1% Pen-Strep in DMEM) at 37 °C for 2 h. The plates were washed twice with PBS and trypsinized. Cells were counted with a hematocytometer and resuspended in freezing media as aliquots (90% FBS, 10% DMSO).

Reprogramming assays

50.000 dH1f cells were transduced with lentiCRISPR gRNA vectors in a medium containing 8 µg/ml protamine sulfate (Sigma-Aldrich)[71] in 12-well plates. 24 h after lentiviral transduction, cells were selected with 1 µg/ml puromycin for 3 days. CRISPR-infected cells were reseeded as 50.000 cells and infected with lentiviral reprogramming factors (pSIN4-CMV-K2M (Addgene plasmid #21164) and pSIN4-EF2-O2S (Addgene plasmid 21162)[72]; 100–250 µl supernatant/virus was used per well (determined empirically for each batch of virus) in a medium containing 8 µg/ml protamine sulfate. At day 6 of reprogramming, cells were trypsinized and re-plated at a 1/8 ratio on 75.000 mitomycin-treated mouse embryonic fibroblasts (mito-MEFs) in 12-well plates. The medium was switched to hES media next day. Media was changed every other day until day fourteen of reprogramming after which media were changed daily until day 21. gRNA sequences used in the reprogramming experiments are listed as Supplementary Table 1 along with their gRNA names. For reprogramming of adult fibroblasts with episomal plasmids in Fig S1C, the following vectors were used: pCXLE-hOCT3/4-shp53-F, Addgene plasmid #27077; pCXLE-hUL, Addgene plasmid #27080; pCXLE-hSK, Addgene plasmid #27078. 1 µg of each plasmid was electroporated into 1 million fibroblasts using Neon transfection system (Thermo). For naïve reprogramming, dH1f cells were grown in fibroblast medium (DMEM, 10% FBS) and seeded at a density of 50,000 cells per well of 12-well plate. Cells were transduced overnight with OSKM viruses. Media was replenished next day and every two days thereafter. On day 7 after OSKM transduction, cells were passaged onto mitomycin-C treated MEFs. On day 9, media was switched to PGXL[73] (1 µM PD0325901, 2 µM XAV939, 2 µM Gö6983, and 10 ng/mL human LIF in N2B27 basal medium) and was replenished every day until day 14. On day 14, cells were fixed using 4% PFA[74].

Immunostaining

Cells were washed with PBS and fixed with 4% paraformaldehyde at room temperature. Biotin conjugated anti-human TRA-1-60 (BioLegend Catalog #330604) was diluted in staining buffer and added onto wells. Plates were incubated overnight at 4 °C on an orbital shaker. Next day, samples were washed with PBS, and Streptavidin-HRP (BioLegend Catalog #405210) secondary antibody in staining buffer was added onto wells. Plates were incubated for 2 h at room temperature. Samples were washed with PBS. The stain was developed with Vector Labs DAB kit at RT. Development solution was washed away with PBS. Cream was added to the wells to provide a contrast for scanning. To quantify naïve PSC colonies, immunostaining with KLF17 antibody (Sigma, HPA024629) was performed.

Quantification of reprogramming efficiency

Tra-1-60-stained plates were scanned, and colony counts were determined by ImageJ. Plates images were converted to 8-bit, single wells were selected using the "Oval" selection tool and copied as a new image. Using "Adjust" and "Threshold" tools, colonies were automatically detected. "Analyze Particles" command was used for counting as well as quantifying total area covered by stained colonies. We used total area covered by TRA-1-60 positive colonies as a measurement of reprogramming efficiency in Fig. 1C to mimic the screen conditions as the enriched gRNAs were measured in sorted cells instead of individual colonies. Additionally, we used this condition to quantify reprogramming efficiency for Fig S1D because individual colonies could not be discerned due to high number of merged colonies. For all other assays, colony counts were used for measuring reprogramming efficiency.

TRA-1-60-PE staining for flow cytometry

Cells were harvested by using 0.05% trypsin and washed in 1X PBS supplemented with 1% FBS. TRA-1-60-PE antibody (BioLegend Catalog #330610) was diluted 1:100 in 1X PBS supplemented with 1% FBS. Samples were incubated on ice for 1 h in a dark condition. Cells were spun washed twice in PBS supplemented with 1% FBS at 1500 rpm for 10 min. Samples were passed through cell strainer flow tubes. BD Accuri C6 Flow Cytometer (BD Biosciences) was used to calculate percentage of stained cells.

Generation of vectors

LentiCRISPRv2 vector was digested with BsmBI (NEB) and gel purified with MN PCR-Clean Up Kit. Extracted plasmids were treated with alkaline phosphatase. 1 µl of each oligo (100 µM) was annealed with T4 Polynucleotide Kinase (3' phosphatase minus, NEB) and T4 DNA Ligase Buffer (NEB) in 10 µl reaction in a thermal cycler with the following settings: 37 °C for 30 min, 95 °C for 4 min and then ramp down to 25 °C at 5 °C/min. Annealed oligos were diluted to 1:200 and used as inserts for cloning. 20 µl ligation reactions were prepared with 50 ng BsmBI-digested, AP-treated vectors, 1 µl of inserts and Quick Ligase (NEB) or T4 DNA Ligase (NEB) in 2X Quick Ligase Buffer or 10X T4 DNA Ligase buffer (NEB), respectively. Ligation reactions were incubated for at least 10 min at RT. 50 µl Stbl3 bacteria were mixed with 5 µl of the ligation reaction and left on ice for at least 5 min (longer durations increased cloning efficiency). Heat shock was applied at 42 °C for 30 s in water bath or 48 °C for 40 s in heat-block and Eppendorfs were placed on ice for 5 min. 150 µl LB was supplemented and cultured in 37 °C at 225 rpm in a shaker for 1 h. 100 µl of the reaction was spread on Ampicillin or Carbenicillin resistance plates. U6 promoter sequencing (Forward sequencing primer for U6 promoter ACTATCATATGCTTACCGTAAC) was used to confirm cloned gRNAs. To create USP22 g1 resistant cDNA, point silent mutation to destroy the NGG site was performed on Flag-HA-USP22 (Addgene plasmid, #22575). To achieve this Q5 site-directed mutagenesis kit was utilized by following manual (NEB, cat. # E0554S). Additionally, point mutations to create K129Q, K129R, and C185A were performed by primers listed on Supplementary Table 2 by Q5 site-directed mutagenesis kit. Mutations were confirmed by Sanger sequencing.

Lentivirus production

HEK 293 T cells were transfected with plasmids encoding the envelope protein (VSVG), Gag-Pol (pUMVC for retroviruses and 8.2DeltaVPR for lentiviruses), and viral vector. FuGENE® 6 Transfection Reagent (Promega) used as a transfection reagent and applied according to the manufacturer's

instructions. After at least 8 h, the transfection medium was replaced with fresh D10 media. Viruses were harvested at 48 and 72 h after transfection and stored at 4 °C. Viral supernatants from the two collections were combined and filtered through a 0.45 µm low protein binding syringe filter to clear viruses from cells and debris. To concentrate the lentiviral supernatants, PEG-8000 (Sigma) was dissolved in 1x PBS to the final concentration of 10% (w/v). Collected and filtered viruses were mixed with 1/5 ratio of PEG and refrigerated overnight. Supernatant/PEG mixture was centrifuged at 1500 g for 30 min at 4 °C. Virus containing pellets were spun down again at 1500 g for 5 min. Pellet was resuspended with 1/10 or 1/100 of the original volume of viral supernatant by using cold 1X PBS. Viruses were aliquoted and stored at −80 °C.

Fluorescence activated cell sorting (FACS)

Cells were harvested by trypsinization and washed at least once time with 1x PBS supplemented with 1% FBS. Same protocol for TRA-1-60-PE staining was performed. BD FACSARIA III was used to sort cells according to manufacturer's instructions.

Library design

gRNAs were designed to target DNA sequences encoding the catalytic or critical domains of chromatin modifiers. DNA sequences of protein domains were manually collected from NCBI Unigene software and CCTop was used to design gRNAs. 3 bp mismatches at off-target sequences were allowed in the 8 bp downstream from 5' end of guideRNA sequences. In the rare cases where no gRNA with these criteria were found, gRNA sequences from GeCKO library that target 5' first coding exon of genes were taken. For each gene, 5–10 gRNAs were designed and 80 non-targeting gRNAs from GeCKO Library were added to the library.

Oligo array synthesis and pooled library cloning

DNA oligonucleotide array was synthesized by the OligoMix (LC Sciences). Oligos harboring homologous arms to target vectors and gRNA sequences were amplified in a 50 µl PCR reaction by mixing 10 µl 5X HF Buffer, 1 µl 10 mM dNTP, 2.5 µl 10 µM forward primer, 2.5 µl 10 µM reverse primer, 0.1 µl oligo mix template, 0.5 µl high-fidelity polymerases and filled with NF water. The lentiCRISPRv2 vector was digested with BsmBI, treated with Antarctic Phosphatase, and gel-purified. Inserts ligated to prepared lentiCRISPRv2 plasmids with Gibson Assembly (NEB) in 1:5 ratio and transformed with Endura™ electrocompetent cells in seven parallel electroporation and plated on large bioassay petri plates (Corning). Total ~1.4 × 10 6 colonies collected from seven plates to have 800x library coverage, and pooled plasmids isolated using maxi-prep kit (Qiagen). GuideRNA regions of isolated plasmids were amplified by PCR to confirm cloning by Illumina Sequencing. Sequencing was performed on a MISeq at MIT BioMicro Center. PCR reaction prepared in 50 µl reactions by mixing 10 µl 5x HF Buffer, 1 µl dNTP (10 mM), 1 µl HF Polymerase, 2 µl forward staggered primer mix, 2 µl reverse primer with index, 10 ng library plasmid pool template.

EpiDoKOL TRA-1-60 screen

20×10^6 dH1f were seeded as 800.000 cells/10 cm plate and library infected with low MOI (~ 0.3). Puromycin selection was applied on day 2 (1ug/ml), and cells were split 1:2 onto 10 cm plates every 4 days. For reprogramming experiments, a total of 8×10^6 dH1f cells (~ 4750 cells/gRNA) were seeded as 600.000 cells/10 cm plate. Cells were treated with 3 µM EPZ004777 for the initial week of reprogramming. For the TRA-1-60 screen, on day 7 of reprogramming, cells were trypsinized and 1/8th of the cells were transferred onto MEF-seeded 10 cm plates for sorting at day 21. At day 21 of reprogramming, cells were spun down at 1500 rpm for 5 min and washed twice with PBS supplemented with 1% FBS. Pellets were resuspended with 2 ml PBS supplemented with 1% FBS. For day 21, TRA-1-60-PE antibody was added at the following 1.5:100 ratio. Two independent biological replicate screens were performed.

Genomic DNA sequencing

Genomic DNA of samples was isolated with MN Nucleospin Tissue kit. 100 µl external and internal PCR reactions were prepared by mixing 2 µl dNTP (10 mM), 1 µl Phusion Polymerase, 20 µl 6X GC Buffer, 5 µl Forward Primer (10 uM), 5 µl Reverse Primer (10 uM), 1 µg gDNA (to ensure at least 100x library coverage) and filled with NF water. For internal PCR reaction, primers were changed accordingly, and 2 µl external PCR product without clean-up directly added instead of 1 µg gDNA. Samples run on a gel and ~350 bp bands were extracted by MN PCR-Clean-up Kit. Samples were sequenced with Illumina HISeq 4000.

Data processing and analysis of next-generation sequencing

The Illumina Sequencing data was trimmed to keep the 20 bp gRNA sequence and aligned to a custom fasta library of the known library sequences using Bowtie. Picards tool was used to quantify relative count of each gRNA from the alignment (BAM) file. sgRNA count tables were analyzed with MAGeCK's *test* function using command-line arguments for replicates (-t replicate1,replicate2 -c replicate1,replicate2) and control sgRNA input[74]. The full list of targeted genes and MAGeCK output for the screen is provided as Supplementary Data 1.

RNA-sequencing

Total RNA was prepared from OSKM-expressing cells as duplicates from sgNT1 and USP22 sg1-expressing cells using Direct-zol kit according to manufacturer's instructions (Zymo Research) including DNase I treatment. RIN scores higher than 6.0 were processed further for library preparation with TruSeq Stranded mRNA (Illumina). Generated libraries were sequenced by Illumina NovaSeq 6000. DESeq2 package was used to identify differentially expressed genes between samples. Rank-ordered gene lists were used for GSEA.

Western blot

Cell pellets were dissolved in lysis buffer (50 mM Tris, pH 7.4, 250 mM NaCl, 5 mM EDTA, 50 mM NaF, 1% Noidet P40, 1 mM PMSF, 1X protease inhibitor and 0.025% NaN_3). Resuspended cells were incubated on ice for 30 min with 10 min vortexing intervals. They were centrifuged at 13,000 rpm for 10 min at 4 °C on a tabletop centrifuge. Supernatant containing whole cell lysate was transferred to a new tube. Protein concentrations were quantified using the Pierce™ BCA Protein Assay Kit (Thermo Fisher Scientific, cat. # 23225) 50 µg of each lysate was incubated at 95 °C for 15 min with 4X Laemmli buffer (Bio-Rad) containing β-mercaptoethanol (Bio-Rad). Boiled samples and protein markers (Bio-Rad, cat. # 161-0374) were loaded onto pre-cast SDS-PAGE gels (Bio-Rad, cat. # 456-1084). Using Bio-Rad trans-blot turbo transfer system at mixed weight transfer settings, proteins were transferred onto PVDF membrane (Bio-Rad, cat. # 1620177), followed by incubation in 5% blotting grade blocker (Bio-Rad, cat. # 1706404) solution for 1 h. Membranes were incubated with antibodies against USP22 (NOVUS, cat. # NBP1-49644), Ubiquityl-Histone H2A (Lys119) (Cell Signaling, cat. # 8240S), Ubiquityl-Histone H2B (Lys120) (Cell Signaling, cat. # 5546S), H2B (Abcam, cat. #ab52599-1:20000), Tubulin and GAPDH (Abcam, cat. #ab9485) at 1:1000 ratio overnight at 4 °C. Next day, membranes were washed with TBS-T for 15 min three times and incubated with secondary antibodies (Abcam, cat. # ab97051 or ab97023) at 1:5000 ratio in blocking solution for 1 h at room temperature. Membranes were washed with TBS-T for 15 min 3 times and incubated shortly with ECL western blotting substrate (Thermo Fisher Scientific, cat. #32209) before imaging using an Odyssey Imaging System (LICOR Biosciences).

Teratoma formation assay

All experiments were carried out under a protocol approved by Koç University Animal Experiments Ethics Committee. Wild-type iPSCs derived from a Caucasian female[52] were cultured in mTeSR Plus media (Stem Cell Technologies, Cat No. 100-0276) on matrigel (Corning, Cat No.07181)

coated plates. Cells were split at ratio 1:20-1:30 and supplemented by ROCK inhibitor Y-27632 was used. Cells were frozen at 10% DMSO in FBS solution. The teratoma formation assay was performed with cells with passage number 55. Mycoplasma tests were performed every two weeks before and after the teratoma injection using the Lonza MycoAlert Detection Kit. iPSCs from 80% confluent 10 cm dish were collected using ReLeSR (Stemcell Technologies) and re-suspended in 100 µl ice-cold 1:1 mixture of Matrigel (Corning) and hES medium. Intramuscular injections were performed in SCID mice. 2 SCID mice per gRNA were used and 1 teratoma from each mouse was analysed. Teratomas were collected 8–10 weeks after injection and analyzed histologically via hematoxylin and eosin staining. Histological sections (2 sections per teratoma) were examined for the presence of differentiation to germ layers with input from Koç University School of Medicine Department of Pathology.

Statistics and reproducibility

Sample size, number of biological and technical replicates, and exact *p*-values are listed in relevant figure legends. Two-sided *t*-tests were used in to calculate *p*-values in Figs. 1C, 1E, 2D. Experiments in Figs. 3E and 4F were repeated twice.

Data availability

RNA-sequencing data are deposited to the NCBI GEO database with the accession number GSE225151. Data used to generate figures are provided as Supplementary Data 1. Uncropped western blots are provided in Supplementary Fig. 5. All other data are available from the corresponding author on reasonable request.

Received: 29 January 2024; Accepted: 6 March 2025;
Published online: 18 March 2025

References

1. Takahashi, K. & Yamanaka, S. Induction of pluripotent stem cells from mouse embryonic and adult fibroblast cultures by defined factors. *Cell* **126**, 663–676 (2006).
2. Takahashi, K. et al. Induction of pluripotent stem cells from adult human fibroblasts by defined factors. *Cell* **131**, 861–872 (2007).
3. David, L. & Polo, J. M. Phases of reprogramming. *Stem Cell Res.* **12**, 754–761 (2014).
4. Liu, X. et al. Reprogramming roadmap reveals route to human induced trophoblast stem cells. *Nature* **586**, 101–107 (2020).
5. Xing, Q. R. et al. Diversification of reprogramming trajectories revealed by parallel single-cell transcriptome and chromatin accessibility sequencing. *Sci. Adv.* **6**, eaba1190 (2023).
6. Li, M. & Izpisua Belmonte, J. C. Deconstructing the pluripotency gene regulatory network. *Nat. Cell Biol.* **20**, 382–392 (2018).
7. Hasegawa, K. et al. Comparison of reprogramming efficiency between transduction of reprogramming factors, cell-cell fusion, and cytoplast fusion. *Stem Cells* **28**, 1338–1348 (2010).
8. Ebrahimi, B. Reprogramming barriers and enhancers: strategies to enhance the efficiency and kinetics of induced pluripotency. *Cell Regen.* **4**, 10 (2015).
9. Plath, K. & Lowry, W. E. Progress in understanding reprogramming to the induced pluripotent state. *Nat. Rev. Genet.* **12**, 253–265 (2011).
10. Brumbaugh, J., Di Stefano, B. & Hochedlinger, K. Reprogramming: identifying the mechanisms that safeguard cell identity. *Development* **146**, dev182170 (2019).
11. Bonnet, J. et al. The SAGA coactivator complex acts on the whole transcribed genome and is required for RNA polymerase II transcription. *Genes Dev.* **28**, 1999–2012 (2014).
12. Baker, S. P. & Grant, P. A. The SAGA continues: expanding the cellular role of a transcriptional co-activator complex. *Oncogene* **26**, 5329–5340 (2007).
13. Daniel, J. A. & Grant, P. A. Multi-tasking on chromatin with the SAGA coactivator complexes. *Mutat. Res.* **618**, 135–148 (2007).
14. Hirsch, C. L. et al. Myc and SAGA rewire an alternative splicing network during early somatic cell reprogramming. *Genes Dev.* **29**, 803–816 (2015).
15. Moraga, F. & Aquea, F. Composition of the SAGA complex in plants and its role in controlling gene expression in response to abiotic stresses. *Front. Plant Sci.* **6**, 865 (2015).
16. Cheon, Y., Kim, H., Park, K., Kim, M. & Lee, D. Dynamic modules of the coactivator SAGA in eukaryotic transcription. *Exp. Mol. Med.* **52**, 991–1003 (2020).
17. Samara, N. L. et al. Structural insights into the assembly and function of the SAGA deubiquitinating module. *Science* **328**, 1025–1029 (2010).
18. Köhler, A., Zimmerman, E., Schneider, M., Hurt, E. & Zheng, N. Structural basis for assembly and activation of the heterotetrameric SAGA histone H2B deubiquitinase module. *Cell* **141**, 606–617 (2010).
19. Bonnet, J., Romier, C., Tora, L. & Devys, D. Zinc-finger UBPs: regulators of deubiquitylation. *Trends Biochem. Sci.* **33**, 369–375 (2008).
20. Melo-Cardenas, J., Zhang, Y., Zhang, D. D. & Fang, D. Ubiquitin-specific peptidase 22 functions and its involvement in disease. *Oncotarget* **7**, 44848–44856 (2016).
21. Lang, G. et al. The Tightly controlled deubiquitination activity of the human SAGA complex differentially modifies distinct gene regulatory elements. *Mol. Cell Biol.* **31**, 3734 LP–3744 (2011).
22. Wang, S. et al. USP22 positively modulates ERα action via its deubiquitinase activity in breast cancer. *Cell Death Differ.* https://doi.org/10.1038/s41418-020-0568-2 (2020).
23. Ling, S. et al. USP22 mediates the multidrug resistance of hepatocellular carcinoma via the SIRT1/AKT/MRP1 signaling pathway. *Mol. Oncol.* **11**, 682–695 (2017).
24. Li, Y. et al. USP22 drives colorectal cancer invasion and metastasis via epithelial-mesenchymal transition by activating AP4. *Oncotarget* **8**, 32683–32695 (2017).
25. Kim, D. et al. Deubiquitinating enzyme USP22 positively regulates c-Myc stability and tumorigenic activity in mammalian and breast cancer cells. *J. Cell Physiol.* **232**, 3664–3676 (2017).
26. Lin, Z. et al. USP22 antagonizes p53 transcriptional activation by deubiquitinating Sirt1 to suppress cell apoptosis and is required for mouse embryonic development. *Mol. Cell* **46**, 484–494 (2012).
27. Li, X. et al. Enzymatic modules of the SAGA chromatin-modifying complex play distinct roles in Drosophila gene expression and development. *Genes Dev.* **31**, 1588–1600 (2017).
28. Koutelou, E. et al. USP22 controls multiple signaling pathways that are essential for vasculature formation in the mouse placenta. *Development* **146**, dev174037 (2019).
29. Sussman, R. T. et al. The epigenetic modifier ubiquitin-specific protease 22 (USP22) regulates embryonic stem cell differentiation via transcriptional repression of sex-determining region Y-box 2 (SOX2). *J. Biol. Chem.* **288**, 24234–24246 (2013).
30. Kosinsky, R. L. et al. Usp22 deficiency impairs intestinal epithelial lineage specification in vivo. *Oncotarget* **6**, 37906–37918 (2015).
31. Arabacı, D. H., Terzioğlu, G., Bayırbaşı, B. & Önder, T. T. Going up the hill: chromatin-based barriers to epigenetic reprogramming. *FEBS J.* **288**, 4798-4811 (2020).
32. Sevinç, K. et al. BRD9-containing non-canonical BAF complex maintains somatic cell transcriptome and acts as a barrier to human reprogramming. *Stem Cell Rep.* **17**, 2629-2642 (2022).
33. Cossec, J.-C. et al. SUMO Safeguards somatic and pluripotent cell identities by enforcing distinct chromatin states. *Cell Stem Cell* **23**, 742–757.e8 (2018).
34. Kolundzic, E. et al. FACT sets a barrier for cell fate reprogramming in caenorhabditis elegans and human cells. *Dev. Cell* **46**, 611–626.e12 (2018).
35. Transcription, M. et al. The RNA polymerase II factor RPAP1 is critical for mediator-driven transcription and cell identity. *Cell Rep.* 396–410 https://doi.org/10.1016/j.celrep.2017.12.062 (2018).

36. Chen, J. et al. The combination of Tet1 with Oct4 generates high-quality mouse-induced pluripotent stem cells. *Stem Cells* **33**, 686–698 (2015).
37. Gao, Y. et al. Replacement of Oct4 by Tet1 during iPSC induction reveals an important role of DNA methylation and hydroxymethylation in reprogramming. *Cell Stem Cell* **12**, 453–469 (2013).
38. Onder, T. T. et al. Chromatin-modifying enzymes as modulators of reprogramming. *Nature* **483**, 598–602 (2012).
39. Sardina, J. L. et al. Transcription factors drive Tet2-mediated enhancer demethylation to reprogram cell fate. *Cell Stem Cell* 1–15 https://doi.org/10.1016/j.stem.2018.11.001 (2018).
40. Liu, Y. et al. CRISPR activation screens systematically identify factors that drive neuronal fate and reprogramming. *Cell Stem Cell* **23**, 758–771 (2018).
41. Michlits, G. et al. CRISPR-UMI: single-cell lineage tracing of pooled CRISPR-Cas9 screens. *Nat. Methods* **14**, 1191–1197 (2017).
42. Yu, J. S. L. et al. CRISPR-knockout screen identifies Dmap1 as a regulator of chemically induced reprogramming and differentiation of cardiac progenitors. *Stem Cells* **37**, 958–972 (2019).
43. Shi, J. et al. Discovery of cancer drug targets by CRISPR-Cas9 screening of protein domains. *Nat. Biotechnol.* **33**, 661–667 (2015).
44. Ozyerli-Goknar, E. et al. Epigenetic-focused CRISPR/Cas9 screen identifies (absent, small, or homeotic)2-like protein (ASH2L) as a regulator of glioblastoma cell survival. *Cell Commun Signal*. **21**, 328 (2023)
45. Ebrahimi, A. et al. Bromodomain inhibition of the coactivators CBP/EP300 facilitate cellular reprogramming. *Nat. Chem. Biol.* https://doi.org/10.1038/s41589-019-0264-z (2019).
46. Breindel, J. L. et al. Epigenetic reprogramming of lineage-committed human mammary epithelial cells requires DNMT3A and Loss of DOT1L. *Stem Cell Rep.* **9**, 943–955 (2017).
47. Lin, Z. et al. Ubiquitin-specific protease 22 is a deubiquitinase of CCNB1. *Cell Discov.* **1**, 15028 (2015).
48. Armour, S. M. et al. A high-confidence interaction map identifies SIRT1 as a mediator of acetylation of USP22 and the SAGA coactivator complex. *Mol. Cell Biol.* **33**, 1487–1502 (2013).
49. Atanassov, B. S. et al. ATXN7L3 and ENY2 coordinate activity of multiple H2B deubiquitinases important for cellular proliferation and tumor growth. *Mol. Cell* **62**, 558–571 (2016).
50. Morgan, M., Ikenoue, T., Suga, H. & Wolberger, C. Potent macrocycle inhibitors of the human SAGA deubiquitinating module. *Cell Chem. Biol.* **29**, 544–554.e4 (2022).
51. Alici-Garipcan, A. et al. NLRP7 plays a functional role in regulating BMP4 signaling during differentiation of patient-derived trophoblasts. *Cell Death Dis.* **11**, 658 (2020).
52. Buganim, Y. et al. Single-cell expression analyses during cellular reprogramming reveal an early stochastic and a late hierarchic phase. *Cell* **150**, 1209–1222 (2012).
53. Bi, Y. et al. Identification of ALPPL2 as a naive pluripotent state-specific surface protein essential for human naive pluripotency regulation. *Cell Rep.* **30**, 3917–3931.e5 (2020).
54. Pastor, W. A. et al. Naive Human Pluripotent Cells Feature a Methylation Landscape Devoid of Blastocyst or Germline Memory. *Cell Stem Cell* **18**, 323–329 (2016).
55. Mikkelsen, T. S. et al. Dissecting direct reprogramming through integrative genomic analysis. *Nature* **454**, 49–55 (2008).
56. Ning, B. et al. USP26 functions as a negative regulator of cellular reprogramming by stabilising PRC1 complex components. *Nat. Commun.* **8**, 349 (2017).
57. Kaemena, D. F. et al. B1 SINE-binding ZFP266 impedes mouse iPSC generation through suppression of chromatin opening mediated by reprogramming factors. *Nat. Commun.***14**, 1–16 (2023).
58. Michlits, G. et al. CRISPR-UMI: single-cell lineage tracing of pooled CRISPR–Cas9 screens. *Nat. Methods***14**, 1191–1197 (2017).
59. Murgai, A. et al. Targeting the deubiquitinase USP7 for degradation with PROTACs. *Chem. Commun.* **58**, 8858–8861 (2022).
60. Guan, J. et al. Chemical reprogramming of human somatic cells to pluripotent stem cells. *Nature* **605**, 325–331 (2022).
61. Liuyang, S. et al. Highly efficient and rapid generation of human pluripotent stem cells by chemical reprogramming. *Cell Stem Cell* **30**, 450–459.e9 (2023).
62. Jani, D. et al. Functional and structural characterization of the mammalian TREX-2 complex that links transcription with nuclear messenger RNA export. *Nucleic Acids Res.* **40**, 4562–4573 (2012).
63. Kopytova, D. V. et al. ENY2: Couple, triple…more? *Cell Cycle* **9**, 479–481 (2010).
64. Naxerova, K. et al. Integrated loss- and gain-of-function screens define a core network governing human embryonic stem cell behavior. *Genes Dev.* **35**, 1527–1547 (2021).
65. Nourreddine, S. et al. A perturbation cell atlas of human induced pluripotent stem cells. *bioRxiv* https://doi.org/10.1101/2024.11.03.621734 (2024).
66. Liu, L. et al. Modeling post-implantation stages of human development into early organogenesis with stem-cell-derived peri-gastruloids. *Cell* **186**, 3776–3792.e16 (2023).
67. Moris, N. et al. An in vitro model of early anteroposterior organization during human development. *Nature* **582**, 410–415 (2020).
68. Jiao, J. et al. Promoting Reprogramming by FGF2 Reveals that the Extracellular Matrix Is a Barrier for Reprogramming Fibroblasts to Pluripotency. *Stem Cells* **31**, 729–740 (2013).
69. Yang J. et al. Unlocking cellular plasticity: enhancing human iPSC reprogramming through bromodomain inhibition and extracellular matrix gene expression regulation. *Stem Cells*. **42**, 706–719 (2024).
70. Collier, A. J. et al. Genome-wide screening identifies Polycomb repressive complex 1.3 as an essential regulator of human naïve pluripotent cell reprogramming. *Sci. Adv.* **8**, eabk0013 (2023).
71. Cornetta, K. & Anderson, W. F. Protamine sulfate as an effective alternative to polybrene in retroviral-mediated gene-transfer: implications for human gene therapy. *J. Virol. Methods* **23**, 187–194 (1989).
72. Yu, J. et al. Human induced pluripotent stem cells free of vector and transgene sequences. *Science***324**, 797–801 (2009).
73. Guo, G. et al. Epigenetic resetting of human pluripotency. *Development* **144**, 2748–2763 (2017).
74. Li, W. et al. MAGeCK enables robust identification of essential genes from genome-scale CRISPR/Cas9 knockout screens. *Genome Biol.* **15**, 554 (2014).

Acknowledgements

We thank Ahmet Kocabay and Ali Cihan Taşkın for help with mouse experiments, and İbrahim Kulaç (Koç University, School of Medicine, Department of Pathology) for examination of histological sections. The authors gratefully acknowledge the use of the services and facilities of the Koç University Research Center for Translational Medicine (KUTTAM), funded by the Presidency of Turkey, Head of Strategy and Budget. This study was supported by an EMBO installation grant to TTO and TUBITAK 1001 project no: 122Z990.

Author contributions

Conceptualization: G.G., K.S., T.T.O. Formal analysis: G.G, K.S., C.A., T.M., N.L., H.S., T.T.O. Investigation: G.G., K.S., C.A., A.Y., A.B.Y., M.G., E.N.E., E.D. Resources: O.C., A.K. Data Curation: K.S., T.M., H.S. Writing—original draft: K.S., T.T.O. Writing—review & editing: All authors. Supervision: T.T.O. Funding acquisition: T.T.O.

Competing interests

The authors declare no competing interests.

Additional information

Supplementary information The online version contains supplementary material available at https://doi.org/10.1038/s42003-025-07899-y.

Correspondence and requests for materials should be addressed to Tamer Önder.

Peer review information *Communications Biology* thanks Angels Almenar-Queralt and the other, anonymous, reviewer(s) for their contribution to the peer review of this work. Primary Handling Editors: Ken-ichiro Kamei and Christina Karlsson Rosenthal.